hydrology

MDPI

Article

Coupled Impacts of Bed Erosion and Roughness Variation on Stage-Discharge Relationships: A 1D Hydrodynamic Modeling Analysis of the Regulated Jingjiang Reach

Yanqing Li, Minglong Dai *, Dongdong Zhang and Yingqi Chen

Department of Water Resources, Bureau of Hydrology, Changjiang Water Resources Commission, Wuhan 430010, China; liyq@cjh.com.cn (Y.L.); zhangdd@cjh.com.cn (D.Z.); chenyq@cjh.com.cn (Y.C.)
* Correspondence: daiml@cjh.com.cn

Abstract

The stage-discharge relationship in the Jingjiang Reach of the Yangtze River has undergone significant alterations due to post-Three Gorges Reservoir (TGR) operation effects, notably bed erosion and roughness variation. This study employs a calibrated 1D hydrodynamic model based on Saint-Venant equations. The model was validated with high accuracy (Nash-Sutcliffe efficiency >0.94 at key stations) using long-term hydrological data (1996–2022). Four scenarios were simulated: pre-dam conditions, post-dam topography with pre-dam roughness, pre-dam topography with increased roughness, and coupled post-dam changes. A novel scenario-based decomposition framework was developed to isolate individual and coupled factor contributions, advancing beyond traditional descriptive approaches. The results indicate that upstream water level changes are mainly controlled by riverbed erosion (e.g., at the Zhicheng Station: the topographic contribution rate exceeds 80% at a flow rate of 5000 m^3/s, resulting in a water level drop of approximately 1.7 m), while downstream, an increase in roughness becomes the dominant factor (e.g., at the Jianli Station: causing a water level rise of about 1.0 m at a flow rate of 13,000 m^3/s, with such changes being particularly pronounced under low-flow conditions). Spatially, topographic influence attenuates downstream, whereas roughness sensitivity amplifies in high-sinuosity reaches (bend coefficient: 3.0). Seasonally, the topographic contribution rate remains stable overall during the low-flow period, e.g., within a narrow range of 0.88–0.98 at Zhicheng Station, while roughness effects exhibit negative values in dry periods (November) due to fine sediment deposition. The coupling effect in mid-discharge ranges (15,000–20,000 m^3/s) at Jianli partially offsets stage reductions. These findings not only provide critical insights for flood forecasting and navigation management in the Jingjiang Reach but also offer a transferable methodology for quantifying hydro-morphodynamic interactions in global regulated rivers, highlighting the model's utility in predictive water resource management.

Keywords: stage-discharge relationship; Jingjiang reach; 1D hydrodynamic modeling; bed erosion; bed roughness; factor contribution; spatial heterogeneity

check for updates

Academic Editor: Ali A. Assani

Received: 17 October 2025
Revised: 18 November 2025
Accepted: 20 November 2025
Published: 22 November 2025

Citation: Li, Y.; Dai, M.; Zhang, D.; Chen, Y. Coupled Impacts of Bed Erosion and Roughness Variation on Stage-Discharge Relationships: A 1D Hydrodynamic Modeling Analysis of the Regulated Jingjiang Reach. *Hydrology* **2025**, *12*, 311. https://doi.org/10.3390/hydrology12120311

Copyright: © 2025 by the authors. Licensee MDPI, Basel, Switzerland. This article is an open access article distributed under the terms and conditions of the Creative Commons Attribution (CC BY) license (https://creativecommons.org/licenses/by/4.0/).

1. Introduction

The stage-discharge relationship is a cornerstone in hydrology, hydraulics, and river engineering [1]. It directly governs the accuracy of flood forecasting, the rationality of water resource allocation, the feasibility of navigation channel maintenance, and the operational safety of hydraulic structures [2]. However, this relationship is not static but dynamically influenced by multiple natural and anthropogenic factors. Globally, numerous river systems

have undergone significant hydro-geomorphic alterations, leading to the gradual obsolescence of historically established stage-discharge relationships [3,4]. This poses persistent challenges and potential risks to practical applications reliant on these relationships [5]. Consequently, a profound understanding of the variation patterns and driving mechanisms of stage-discharge relationships holds universal significance for enhancing the scientific rigor and predictive capability of river management.

The Jingjiang Reach, a pivotal segment of the middle Yangtze River, profoundly influences flood control, navigation, and ecological security across the entire basin through its hydrological regime and channel evolution [6–8]. In recent years, driven by the operation of the TGR and upstream cascade reservoirs, the Jingjiang Reach has experienced pronounced clear-water scouring and incision, resulting in widespread bed-level lowering and cross-sectional reshaping [9]. Concurrently, systematic alterations in bed roughness may arise from changes in bed material composition, sand wave morphology, and vegetation coverage [10,11]. The coupling effects of topographic incision and roughness variation inevitably exert complex and far-reaching impacts on the longitudinal stage-discharge relationships along the Jingjiang Reach, necessitating systematic investigation. The operation of the Three Gorges Dam has not only altered the hydrological regime in the lower Yangtze River, such as increased low flows and an earlier dry season, but has also significantly impacted the transport of suspended sediment and the geomorphic dynamics of riverine sandbars. These adjustments exhibit characteristics of a lagged response [12–14]. The challenges faced by Jingjiang are not isolated; many reservoir-regulated or intensively human-modified rivers worldwide—such as the lower Mississippi River (USA), the Rhine River (Europe), and the Nile River (Egypt)—have undergone or are undergoing similar channel adjustments, leading to significant shifts in their stage-discharge relationships [15–18]. These cases underscore the broad necessity and urgency of studying such issues.

Substantial research efforts have been devoted to understanding stage-discharge relationship variations. Theoretically, hydraulic principles reveal that stage-discharge relationships are governed by flow cross-sectional geometry (morphology) and flow resistance (roughness) [19,20]. Practically, field observations, physical model experiments, and numerical simulations are commonly employed to elucidate variation patterns [1,21]. Numerical modeling, particularly 1D hydrodynamic models, has emerged as a mainstream tool for analyzing the stage-discharge relationship changes in complex river systems due to its efficiency in simulating long-term flow dynamics and channel evolution over extended reaches [22]. For instance, 1D models have been extensively applied in managing rivers like the lower Colorado and Rhine to predict post-dam stage reduction and flow relationship shifts, providing critical foundations for adaptive management strategies [23–25]. These studies offer essential methodological references and contextual knowledge for addressing analogous issues in the Jingjiang Reach.

Despite significant progress, key gaps persist in the quantitative attribution analysis of stage-discharge relationship changes in the Jingjiang Reach. First, topographic incision (increasing flow area) and bed roughness variation (affecting flow resistance) often occur simultaneously and interactively. Their contributions to stage-discharge relationship changes—and the spatiotemporal (longitudinal and discharge-dependent) distribution of these contributions—remain inadequately quantified [26]. Second, existing Jingjiang-focused studies often emphasize single factors or localized reaches, lacking a systematic simulation framework that integrates the coupling effects of topographic and roughness changes across the entire reach under a unified 1D hydrodynamic model. Furthermore, accurately characterizing and simulating the dynamic evolution of bed roughness under clear-water scouring conditions, and effectively incorporating it into 1D models, constitutes a critical challenge for prediction accuracy [27,28]. Global experiences indicate that ne-

glecting such coupling effects or mishandling roughness dynamics may lead to significant deviations in predicting stage reduction magnitudes or flow relationship trends [29].

Therefore, this study employs a 1D hydrodynamic model to systematically investigate the influence of topographic incision and bed roughness variation on longitudinal stage-discharge relationships in the Jingjiang Reach. Key research components include: (1) developing and calibrating a 1D hydrodynamic model tailored for the Jingjiang Reach; (2) designing and simulating scenarios (e.g., isolated topographic incision, isolated roughness change, coupled effects); (3) quantifying individual and coupled contributions of incision and roughness changes to stage-discharge relationship variations at different longitudinal positions and discharge levels; (4) revealing spatial distribution patterns and discharge-dependent influence mechanisms. This work holds dual significance: practically, it provides direct scientific support for Jingjiang's flood control (e.g., refined stage forecasting), navigation management (e.g., channel depth assurance), water resource allocation, and post-assessment of the TGR; theoretically, it enriches fluvial hydrodynamics by elucidating the coupling mechanisms and quantitative contributions of topography-roughness interactions, offering transferable methodologies for global alluvial rivers facing similar challenges under large reservoir impacts.

2. Methodology and Materials

2.1. Study Area

The Jingjiang Reach of the Yangtze River (from Zhicheng to Luoshan) serves as the core study area, spanning approximately 339 km (Figure 1A). It constitutes a critical transitional zone between the TGR Region and the Jianghan-Dongting Plains. Bounded by Xinchang, the reach is divided into the Upper Jingjiang (Zhicheng–Xinchang), characterized as a slightly sinuous anabranching channel (sinuosity index 1.7), and the Lower Jingjiang (Xinchang–Chenglingji), renowned as a highly meandering channel (sinuosity index 3.0). The segment from Chenglingji to Luoshan (including the Jiepai reach) is characterized as a relatively straight anabranching channel. Within an 80-km straight-line distance, it develops 16 major river bends. Key hydrological stations along the reach include: Zhicheng Station (benchmark for TGR outflow monitoring), Shashi Station (Located in the transition zone between the Upper Jingjiang Reach and the Lower Jingjiang Reach, where the bend sinuosity index increases from 1.7 to 3.0; this area can effectively capture the spatial gradient characteristics of the hydrodynamic response to riverbed incision and changes in roughness), Jianli Station (representative bend monitoring point), and Luoshan Station (eastern boundary node interacting with Dongting Lake).

Following the TGR impoundment, Lower Jingjiang experienced a 23% increase in the flow area of the bankfull channel (Figure 1B). However, the Jiepai section near Luoshan still exhibits intense lateral migration. This reach safeguards 733,000 hectares of farmland and tens of millions of residents in the Jianghan Plain. Against the backdrop of annual sediment load plummeting from 462 million tons to 86 million tons, it stands as an ideal research sample for investigating cross-sectional stage-discharge relationship evolution under anthropogenic influences.

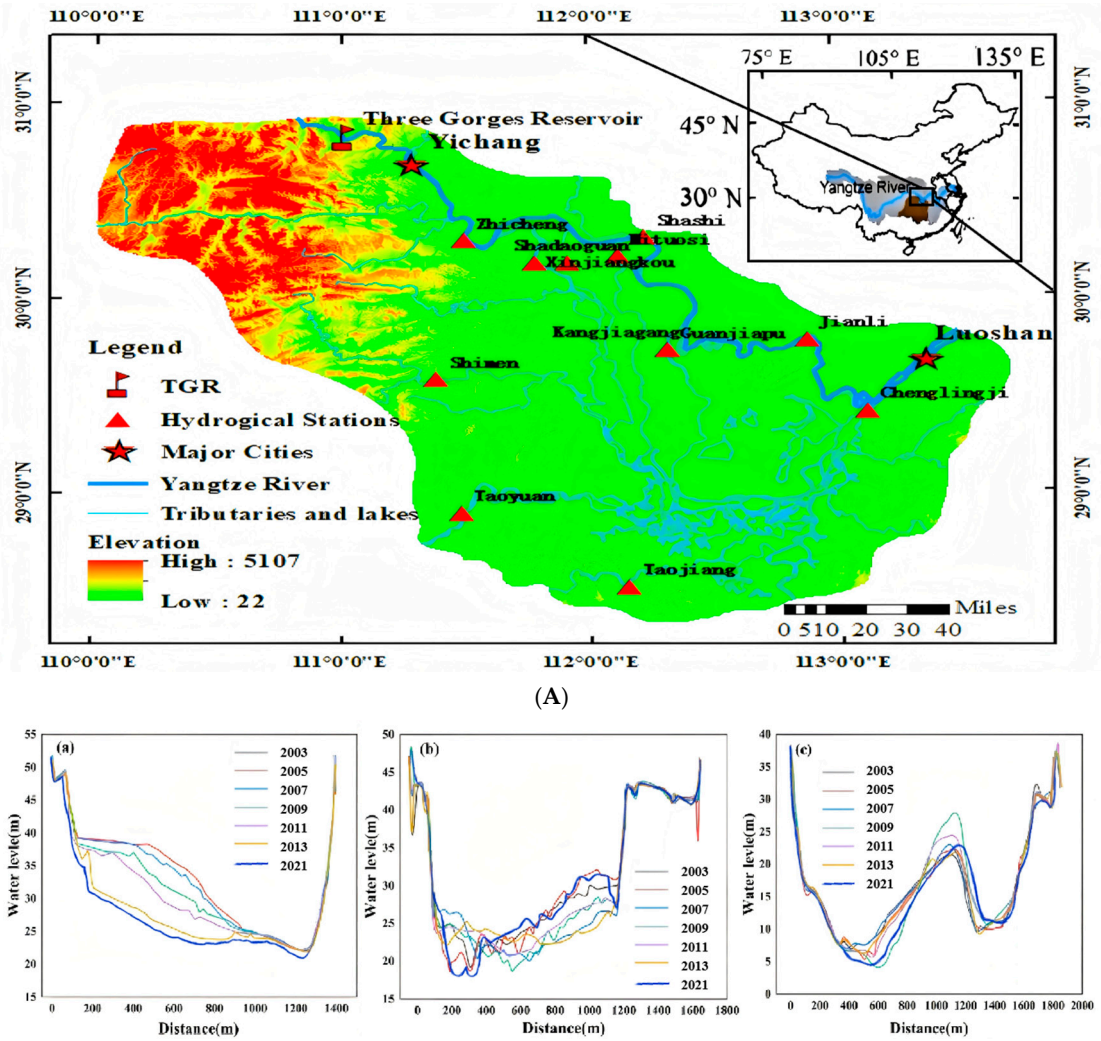

(**A**)

(**B**)

Figure 1. (**A**) Digital Elevation Model (DEM) of the Jingjiang Reach, (**B**) Evolution of Typical Cross-Section Morphology, (**a**) Zhicheng, (**b**) Shashi, (**c**) Luoshan.

2.2. One-Dimensional Hydrodynamic Model Framework

The 1D hydrodynamic modeling framework (DHI Mike 11) adopted in this study is constructed based on the Saint-Venant equations, whose mathematical formulation comprises the continuity equation and momentum equation [30]:

$$\frac{\partial A}{\partial t} + \frac{\partial Q}{\partial x} = ql \tag{1}$$

$$\frac{\partial Q}{\partial t} + \frac{\partial}{\partial x}\left(\frac{Q^2}{A}\right) + gA\frac{\partial h}{\partial x} + g\frac{Q|Q|}{C^2AR} = 0 \tag{2}$$

where A denotes the cross-sectional area (m^2), Q is the discharge (m^3/s), h is the water depth (m), g is the gravitational acceleration (m/s^2), C is the Chezy coefficient (dimensionless), R is the hydraulic radius (m), and ql presents the lateral inflow (m^2/s). This system of equations is discretized using the Preissmann implicit difference scheme with a fully implicit weighting coefficient ($\theta = 1$) to enhance numerical stability. Spatial discretization employs a uniform grid with a cross-section spacing of 500 m, while the temporal step is dynamically adjusted between 300 s and 600 s to balance computational efficiency

and accuracy. The solution is achieved via a pentadiagonal matrix solver for efficient iterative computation.

Boundary conditions were processed using hybrid inputs: the upper boundary employed a time-series discharge hydrograph (e.g., discharge regulated by the TGR), while the lower boundary utilized a stage-discharge relationship curve at Luoshan Station. Tributary boundaries were defined by stage-discharge curves from observational stations (Xinjiangkou, Shadaoguan, Mituosi, Guanjiapu, and Kangjiagang) as outflow conditions. To address the complex geomorphology of the Jingjiang Reach, the model integrated 527 surveyed cross-sectional datasets. GIS technology extracted key morphological parameters, including the width-depth ratio and sinuosity index (Upper Jingjiang: 1.7; Lower Jingjiang: 3.0), and incorporated dynamic roughness coefficients (0.027–0.035) to reflect bed coarsening effects.

The simulation accuracy of the model was quantitatively evaluated by referencing the model accuracy evaluation grading criteria adopted in the study by Moriasi et al. (as shown in Table 1) [31]. Model performance was validated using observed data from Zhicheng, Shashi, and Luoshan stations (Figure 2), with accuracy evaluated via the Nash-Sutcliffe efficiency coefficient (NSE) [32,33] and relative error (RE). During both the calibration and validation periods, all three stations achieved NSE values exceeding 0.75 and absolute RE values below 10%. According to the criteria in Table 1, these results consistently place the model's performance in the "Excellent" grade. Specifically, Calibration results showed NSE values of 0.99, 0.99, and 0.98 for Zhicheng, Shashi, and Luoshan stations, respectively; the maximum errors between the measured and simulated flow rates were 1144 m^3/s, 1650 m^3/s, and 2090 m^3/s for the three stations. During validation, NSE reached $\geq$0.99 at all stations, with RE values of 1.36%, 1.36%, and 2.27%. For annual extreme values, most relative errors of peak discharge and stage were controlled within 10% (e.g., Luoshan's maximum discharge error: −9.20% during calibration). These results demonstrate the model's high precision in simulating hydrological processes within the Jingjiang Reach, laying a robust foundation for subsequent research.

Table 1. Classification of Evaluation Metrics for Model Simulation Performance.

Grade	NSE	RE (%)
Excellent	$0.75 < NSE \leq 1.00$	$\|RE\| < 10$
Good	$0.65 < NSE \leq 0.75$	$10 \leq \|RE\| < 15$
Pass	$0.50 < NSE \leq 0.65$	$15 \leq \|RE\| < 25$
Fail	$NSE \leq 0.50$	$\|RE\| \geq 25$

The statistical results of the Nash-Sutcliffe efficiency coefficient (NSE) and mean relative error (MRE) for each station along the mainstream are presented in Table 2. It can be observed that: All stations achieved NSE values above 0.94, indicating high fitting accuracy. The MRE at each station remained within 2.66%. Overall, the model performance during the validation period surpassed that of the calibration period. According to the evaluation criteria grades for model simulation effectiveness in Table 2, all stations attained an "excellent" rating for both NSE and MRE metrics.

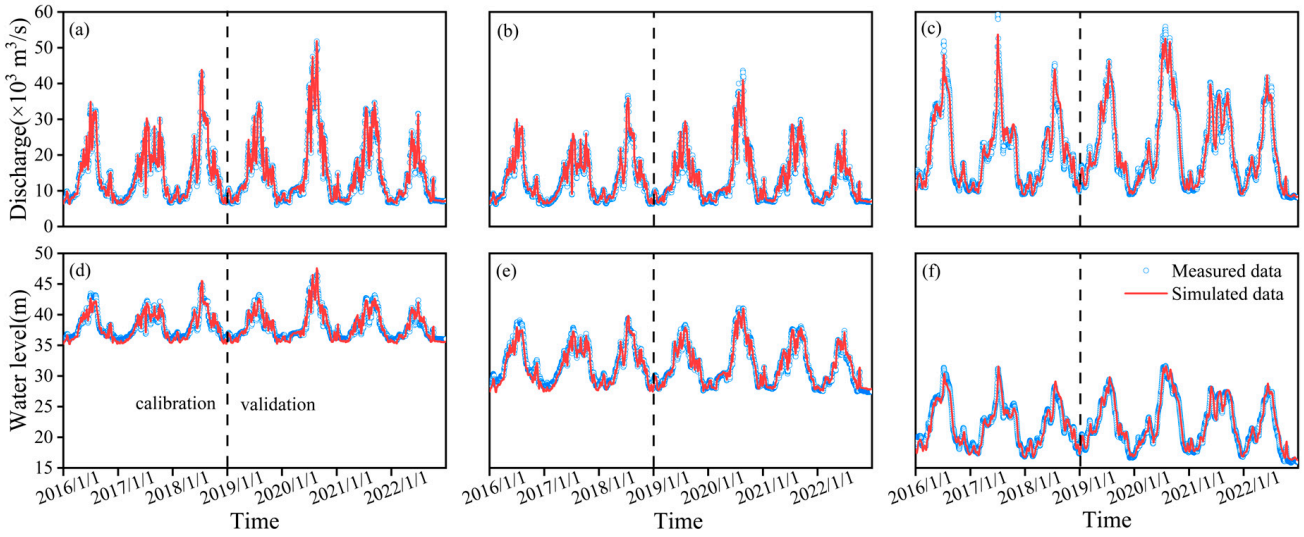

Figure 2. Calibration and Validation Results of the 1D Hydrodynamic Model. (**a**) Zhicheng Discharge, (**b**) Shashi Discharge, (**c**) Luoshan Discharge, (**d**) Zhicheng Water level, (**e**) Shashi Water level, (**f**) Luoshan Water level.

Table 2. Goodness-of-fit test for observed data at each station.

Gauging Stations		Zhicheng	Shashi	Luoshan
Calibration	Nash-Sutcliffe efficiency coefficient (NSE)	0.99	0.99	0.98
	Relative error (%)	1.32	2.66	1.49
Validation	Nash-Sutcliffe efficiency coefficient (NSE)	0.99	0.99	0.99
	Relative error (%)	1.36	1.36	2.27

2.3. Multi-Period Data Collection

The multi-period dataset adopted in this study integrates hydrological sequences and topographic spatial data, encompassing complete cycles before and after the impoundment of the TGR.

The primary hydrological data comprise daily average water level and discharge observations (1996–2002: pre-dam; 2003–2022: post-dam) from key control stations—Yichang, Zhicheng, Shashi, Jianli, and Luoshan—along the Jingjiang River reach. These data, sourced from the routine monitoring system of the Changjiang Water Resources Commission (CWRC) Hydrology Bureau, underwent continuity checks (missing rate < 0.1%) and hydrological consistency correction (removing non-natural fluctuations induced by sluice operations). Observations from 1996 to 2010 fused manual measurements with automatic water level recorders, while post-2011 data utilized GNSS positioning and ADCP online discharge measurement systems. Topographic data comprise: (1) 1996 full-channel DEM (10 m resolution, vertical RMSE: ±0.8 m); (2) 2021 fused LiDAR and multi-beam bathymetry (0.5 m resolution, vertical accuracy: ±5 cm), both acquired by the CWRC Survey Bureau through fixed-section monitoring and long-range channel surveys. The two-phase data were validated for erosion/deposition residuals via Cloud-to-Cloud (C2C) algorithms ($R^2 > 0.91$), with spatial standards unified via control-point coordinate transformation (WGS-84 registration residual < 0.1 m). This dataset comprehensively supports research on the time-dependent mechanisms by which bed deformation and roughness variation impact stage-discharge relationships. The streamflow data of tributaries were obtained from

the daily average discharge records (2003–2022) of the following hydrological stations: Shimen, Taoyuan, Taojiang, Xiangtan, and Changyang. Topographic data were derived from surveyed terrain measurements in 1996 (pre-impoundment) and 2021 (post-impoundment).

Furthermore, to align with the core objective of this study—to quantify the net contribution of bed degradation and roughness variation to the stage-discharge relationship—the boundary conditions of the model were set as follows: the downstream boundary employed the stage-discharge rating curve at the Luoshan Station, which inherently incorporates the average backwater effect of Dongting Lake. The diversion processes at internal network nodes (e.g., Songzikou and Taipingkou) were not preset as constant values but were automatically calculated by the MIKE 11 HD model through hydraulic computation based on the surveyed topography (1996 or 2021) for each scenario. This approach ensures a consistent basis for inter-period scenario comparison by rationally reflecting the changes in diversion capacity caused by topographic evolution itself, thereby effectively isolating the impacts of the key driving factors.

2.4. Scenario Design

The scenario design framework of this study focuses on the evolution mechanism of stage-discharge relationships in the Jingjiang Reach (Table 3). Topographic change scenarios were constructed based on two-phase surveyed terrain data (1996 and 2021) from the CWRC Hydrology Bureau. For roughness variation scenarios, Manning's n values were assigned according to geomorphic evolution characteristics: based on model calibration results, the bed roughness in 1996 ranged from 0.023 to 0.028, whereas after decades of TGR operation, the composite roughness of the channel in 2021—considering bed scouring and coarsening—ranged from 0.027 to 0.035.

Table 3. Research scenarios of the Jingjiang reaches.

Ro\Topo	**D1**	**D2**
n1: 1996 Roughness	Scenario 1: Baseline (1996 Topo. + 1996 Rough.)	Scenario 2: Topography Change (2021 Topo. + 1996 Rough.)
n2: 2021 Roughness	Scenario 3: Roughness Change (1996 Topo. + 2021 Rough.)	Scenario 4: Combined Effect (2021 Topo. + 2021 Rough.)

It should be noted that this study aims to reveal long-term evolutionary patterns by comparing the topography and roughness between two typical years (1996 and 2021). The water level changes discussed herein are the results calculated under the specific scenarios described above. It is noteworthy that field observations indicate the maximum post-TGR water level decline in the Jingjiang Reach occurred at the Shashi Station, exceeding 2.0 m.

Ro denotes the bed roughness, and Topo represents the bed topographies.

This study establishes a water level increment decomposition model to analyze the impacts of bed erosion and roughness variation, based on a comparison of four distinct scenarios: a baseline scenario (Scenario 1) using 1996 topography and 1996 roughness; a scenario examining only topographic change (Scenario 2) with 2021 topography and 1996 roughness; a scenario examining only roughness change (Scenario 3) with 1996 topography and 2021 roughness; and a final scenario (Scenario 4) that evaluates the combined effect of both 2021 topography and 2021 roughness.

In the calculation of factor contribution rates, Shashi and Jianli Stations were selected as key nodes. The stratified difference method was employed to decouple the perturbation effects of topography and roughness on water level variations along the mainstream. The topographic influence was quantified as $\Delta Zt = ZX1 - ZX2$, reflecting the water level decline induced by bed erosion, while the roughness influence was quantified as

ΔZn = ZX1 − ZX3, representing the water level rise caused by bed coarsening. The total influence was defined as ΔZtotal = Σ(ΔZt + ΔZn). Through FAST (Fourier Amplitude Sensitivity Test) verification, the contribution rates of each dominant factor to channel water level changes were analytically determined. This methodology effectively isolates multi-factor coupling effects, providing quantitative foundations for studying the bed evolution-hydraulic response mechanism under the influence of the TGR.

3. Results

3.1. Variation in Stage-Discharge Relation

Figure 3 intuitively reveals the compound impacts of topographic and roughness changes on the hydrological characteristics at Zhicheng Station before and after the impoundment of the TGR, by comparing stage-discharge relationship curves under four computational scenarios. Under identical discharge conditions, the divergence between Scenario 1 (pre-dam topography with original roughness) and Scenario 2 (post-impoundment topography with maintained original roughness) demonstrates that post-reservoir topographic adjustments significantly reduce water stage elevations in the medium-low flow range (5000–20,000 m^3/s). For instance, at 5000 m^3/s, the Scenario 2 water stage decreases by approximately 1.7 m compared to S1, indicating that bed erosion and enlarged flow cross-section enhance channel conveyance capacity. The effect of roughness parameter adjustment is particularly pronounced in the comparison between Scenario 3 (pre-dam topography + increased roughness) and Scenario 1, where roughness augmentation systematically elevates stages by 0.4–1.0 m under equivalent discharges, signifying that increased roughness enhances flow resistance. Notably, the curve of Scenario 4 (post-impoundment topography + increased roughness) is positioned between S2 and Scenario 3, revealing that roughness increase due to bed coarsening partially offsets the stage-reduction effect from topographic adjustments. Under their combined influence, stages for discharges below 10,000 m^3/s remain approximately 1.0 m lower than the pre-impoundment baseline (Scenario 1). Differences in confidence bands and prediction bandwidths among scenarios indicate narrower uncertainty ranges for polynomial fitting under post-impoundment topographic conditions, potentially stemming from field measurements better aligning with modern channel morphology. Collectively, this set of curves quantitatively deconvolves the coupling mechanism by which engineering-induced topographic evolution and anthropogenic roughness adjustments affect stage-discharge relationships, providing a scientific basis for assessing the impact of TGR operations on flood control operations in the middle Yangtze reaches.

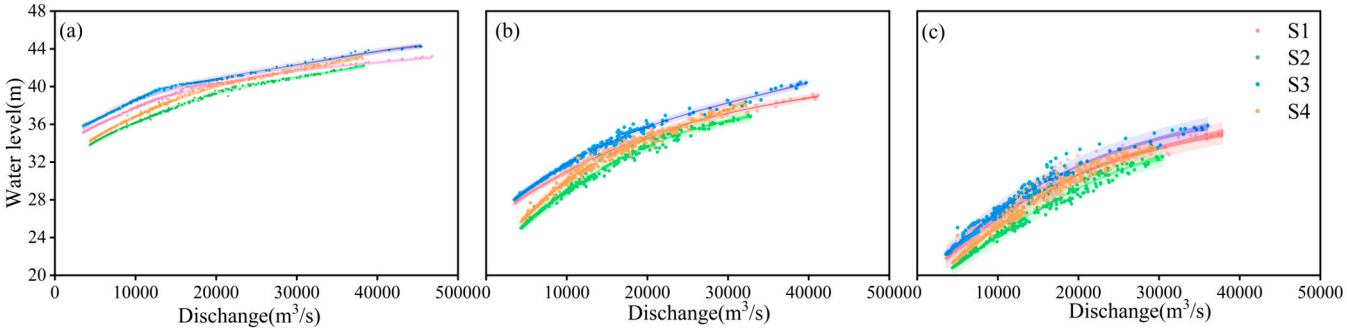

Figure 3. Comparison of Stage-Discharge Relationships under Computational Scenarios. (**a**) Zhicheng, (**b**) Shashi (**c**) Jianli.

By comparing the stage-discharge relationship curves at Zhicheng, Shashi, and Jianli stations, it is evident that the topographic and roughness adjustments induced by the

TGR impoundment exert spatially heterogeneous impacts on the middle Yangtze reaches. From upstream Zhicheng to downstream Jianli, the stage-reduction effect from topographic adjustments shows a decreasing trend: At Zhicheng Station, the water level at a discharge of 8000 m^3/s under Scenario 2 decreased by 1.45 m compared to the pre-impoundment period, and its stage-discharge relationship curve exhibits a converging trend, indicating that the riverbed erosion effect tends to saturate with increasing flow. While at Shashi Station, the reduction diminishes to 1.3 m under the same discharge, though the shapes of the stage-discharge curves before and after topographic adjustments are more similar. At Jianli Station, Scenario 4 (incorporating roughness increase) narrows the stage reduction further to 0.4 m, reflecting the downstream attenuation of bed erosion intensity, likely associated with reduced channel slope and diminished sediment transport capacity.

Conversely, the response to roughness changes exhibits inverse spatial characteristics: At Zhicheng Station, the Scenario 3 roughness increase leads to a relatively large rise in water level during low-flow periods (approximately 0.9 m). Increases to 1.0 m at Shashi, and reaches 1.1 m at Jianli under 10,000 m^3/s, indicating heightened roughness sensitivity in downstream reaches, potentially due to higher channel sinuosity and more complex thalweg-bar morphology in the Jianli segment.

The divergence of Scenario 4 curves (post-impoundment topography + roughness increase) across stations reveals the longitudinal evolution of compound effects: at Zhicheng and Shashi, topography-dominated adjustments maintain stages below pre-impoundment baselines, whereas at Jianli, the two effects nearly offset each other in the medium-discharge range (15,000–20,000 m^3/s). Spatial differences in confidence bandwidths are equally pronounced: post-impoundment prediction bands narrow to 0.4 m at Zhicheng but remain at 0.8 m and 1.2 m at Shashi and Jianli, respectively, reflecting higher hydrological uncertainty downstream, likely influenced by complex hydrodynamic factors such as Dongting Lake backwater effects and tributary inflows.

This longitudinal gradient response mechanism underscores that the hydrological reconfiguration driven by the TGR exhibits significant reach-specificity in the middle Yangtze, necessitating spatially differentiated stage-discharge forecasting models for flood control operations.

3.2. Factor Contribution Decomposition

From the perspective of terrain change factors, the driving mechanisms of water level variations at Zhicheng, Shashi, and Jianli stations exhibit significant longitudinal differentiation, demonstrating upstream-dominated and downstream-complex response characteristics. Figure 4 visually captures the spatiotemporal shift in the dominance of topographic influence through distinct rose diagram patterns. Upstream at Zhicheng Station (Figure 4a), the topographic contribution rate from January to December exhibits a consistently high and stable pattern throughout the year, with a median value of 0.94. The monthly values are densely distributed within a narrow range of 0.91 to 0.98, indicating that water level changes at this station are almost entirely controlled by riverbed erosion, with minimal influence from seasonal fluctuations. This reflects the persistence and stability of clear-water scour effects in the reach immediately downstream of the dam. In contrast, a clear transition in the dominant controlling factor is observed at the mid-stream station. At Shashi Station (Figure 4c), the median contribution rate decreases significantly to 0.72. This graphical feature signifies a temporary shift in dominance, where the influence of topographic changes is surpassed by other factors (e.g., instantaneous hydrological events or roughness variations) during the flood season. The contribution rate ranges between 0.94 and 1.02 from January to March, declines to approximately 0.72 in June, turns negative during July-August, rises to about 1.68 in September–October, and shows a brief

decline in November before increasing again. The data distribution expands substantially (−0.34 to 1.68), demonstrating a notable weakening of its influence and increased uncertainty. At Jianli Station (Figure 4e), the magnitude and temporal trend of the monthly contribution rate are highly similar to those at Shashi Station, but the attenuation is more pronounced. The median value further decreases to 0.65, with fluctuations maintained within the range of −0.25 to 1.58. The contribution rate of terrain changes demonstrates certain similarities across stations and months, such as higher values in specific periods (e.g., September–December). The identical contribution rates at Shashi and Jianli stations may be attributable to their greater distance from the TGR, rendering their hydrological responses more dependent on seasonal factors (e.g., precipitation, discharge) in shaping terrain dynamics.

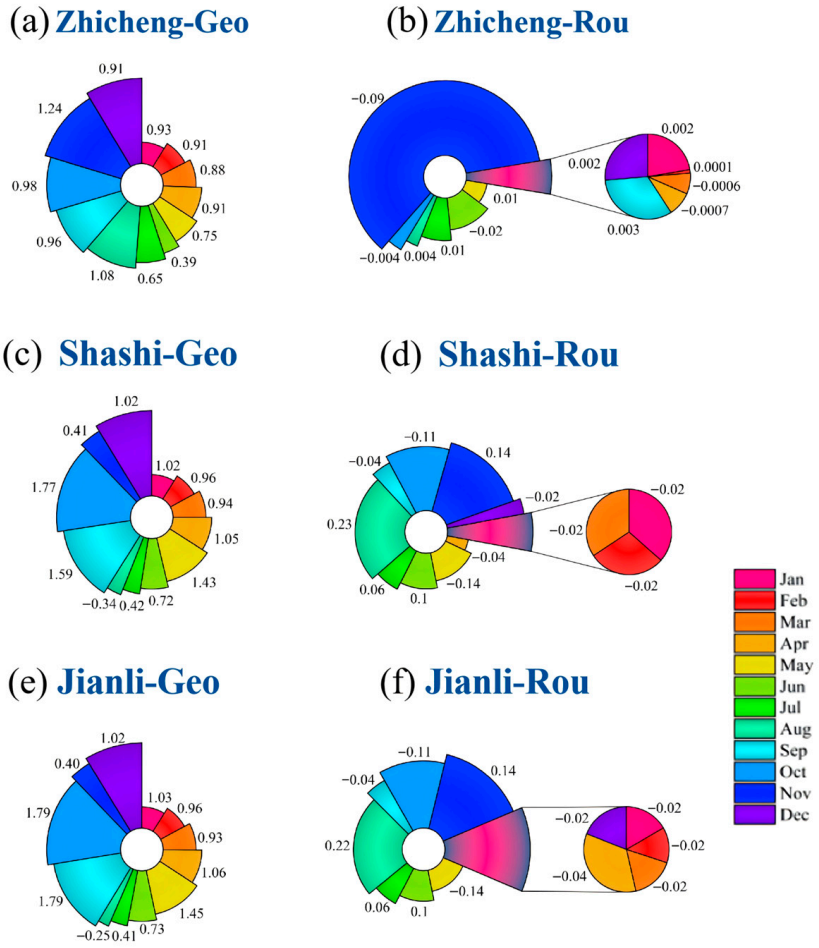

Figure 4. Rose diagram of contribution rates for key influencing factors at each station, where (**a**,**b**) correspond to the two influencing factors of topographic change and roughness change at Zhicheng Station, (**c**,**d**) correspond to the two influencing factors of topographic change and roughness change at Shashi Station, and (**e**,**f**) correspond to the two influencing factors of topographic change and roughness change at Jianli Station.

From the perspective of roughness change factors, the contribution rate at Zhicheng Station (Figure 4b) fluctuates mostly between −0.1 and 0.01 across months, during the dry season, the contribution rate of the monthly variation factor is relatively small, close to zero, indicating that the influence of roughness on water level is weak during this period; the extreme value of the contribution rate occurs in November, reaching −0.09, reflecting a certain negative regulatory effect of roughness on water level during the low-water stage in late autumn. In contrast, the radar charts for Shashi Station (Figure 4d) and

Jianli Station (Figure 4f) exhibit strikingly similar, more symmetrical shapes, indicating a shared seasonal pattern of roughness influence in the middle and lower reaches that is fundamentally different from the upstream station. Both show smaller values from January to March and relatively larger values in other months, demonstrating strong consistency with the influence patterns of terrain change factors. The contribution rate of roughness change also displays analogous fluctuation trends across stations, though its absolute values are comparatively smaller. This indicates that roughness changes exert a weaker influence on these stations than terrain changes, yet still follow distinct seasonal variation patterns—such as lower values in specific months—likely associated with factors like flow velocity and water level affecting roughness.

3.3. Spatial Heterogeneity Analysis

The spatiotemporal response patterns visualized in Figure 5 reveal a clear shift in the dominant mechanisms driving water level changes, both seasonally and along the river course. From the perspective of spatiotemporal response characteristics of topographic changes, Zhicheng Station exhibits significant seasonal differentiation and spatial gradients. At Shashi and Jianli stations, annual terrain contribution values are consistently positive (Shashi contribution rates range from 0.2 in September to 1.6 in January; Jianli from 0.5 in September to 2.8 in October), indicating that channel morphological adjustments dominate water level changes in the middle-lower reaches, likely associated with cross-section contraction due to sediment deposition. In contrast, the radar chart for Zhicheng Station shows unique negative responses during this period (October: −4.6 to December: −4.4), forming a distinct inward depression on the plot, which reveals that in the upstream reach, the water-level reduction effect induced by channel widening exceeds the impact of topographic changes themselves, influenced by Dongting Lake's backwater effect. Spatially, the attenuation of topographic influence intensity along the river course is pronounced: the minimum positive contribution rate at Jianli Station (0.5 in September) is four times higher than at Zhicheng Station (0.1 in September), corroborating that hydrodynamic processes intensify upstream.

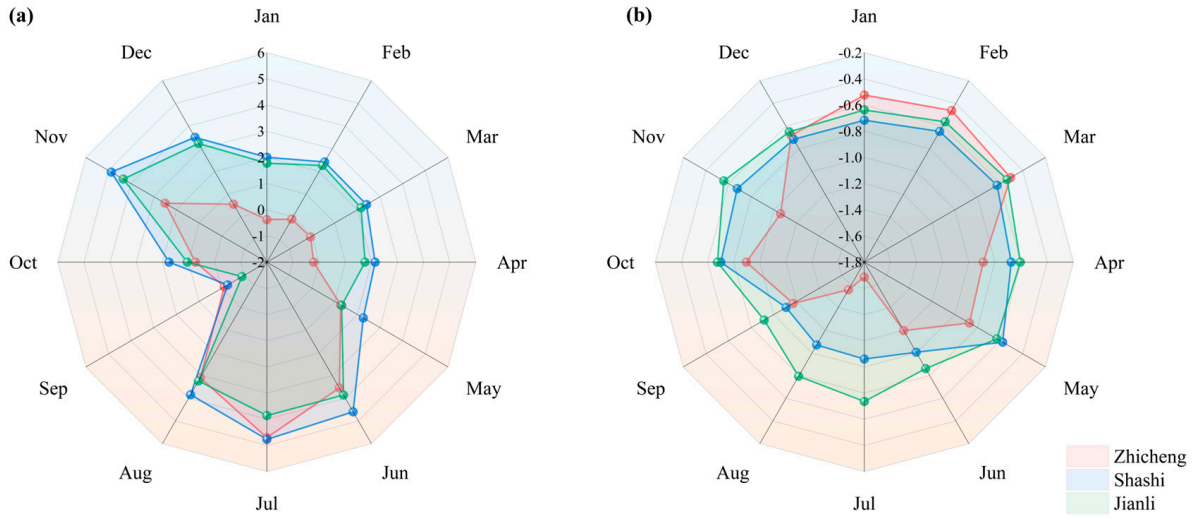

Figure 5. Response of Water Level at the Site to Changes in Riverbed Topography and Roughness Coefficient. (**a**) Topographical changes, (**b**) Roughness changes.

The water level response to roughness changes demonstrates stronger seasonal synchrony and spatial heterogeneity, which is vividly captured in Figure 5b. All three stations exhibit response peaks from September to October, as seen by the outward bulge in their

respective contours during these months, yet Zhicheng Station shows drastic fluctuations in roughness contribution rates from September to December (ranging from −0.7 in November to 5.6 in October), reflecting dynamic adjustments of coarse-grained bed materials under dry-season sedimentation in the upstream reach, resulting in an amplifying effect of bed resistance changes on water levels. Although Shashi and Jianli stations share synchronized trends, their contribution rates decrease concurrently (Shashi: −0.7 in October; Jianli: −1.8 in October), as indicated by their contours lying closer to the center for most months compared to Zhicheng's, which suggests that fine-grained sediment buffering in the middle-lower reaches diminishes roughness sensitivity. Notably, except for September, roughness changes at Shashi and Jianli stations yield negative contributions to water levels, potentially related to abrupt roughness shifts caused by unique bed morphology during ice-run periods. Such extreme responses vanish entirely at downstream stations, highlighting the nonlinear modulation of geographic location on hydrodynamic parameter transmission processes.

4. Discussion

This study quantitatively analyzes the evolution mechanism of the stage-discharge relationship in the Jingjiang River reach through a 1D hydrodynamic model, revealing that the coupling effects of bed erosion and roughness changes exhibit significant spatiotemporal heterogeneity. Topographic changes contribute over 80% to water level reduction at the upstream Zhicheng Station (e.g., as in the low-flow period, the water level drop reaches 1.7 m, and its contribution rate gradually converges with increasing discharge), while this contribution attenuates downstream to less than 50% at Jianli Station, directly linked to the weakening of bed scour intensity and reduced sediment transport capacity due to decreasing channel slope. Notably, the influence of roughness changes follows a reverse spatial pattern: Due to the high sinuosity (with a bend ratio of 3.0) and complex shoal-channel morphology at the downstream Jianli Station, the adjustment of roughness plays a particularly prominent role in regulating the range of water level fluctuations, which is significantly stronger than that in the upstream reach, confirming enhanced flow resistance sensitivity under complex boundary conditions.

Seasonal dynamics further highlight hydrological regulation. The topographic contribution rate exhibits a downstream attenuation pattern spatially, with median values of 0.94, 0.72, and 0.65 at Zhicheng, Shashi, and Jianli stations, respectively. Meanwhile, downstream stations show an expanded fluctuation range and the emergence of negative values, reflecting a response pattern where the controlling effect of topography gradually weakens downstream, while the influence of local erosion and deposition intensifies. While roughness contributions turn negative in dry seasons (November) at Shashi and Jianli Stations, likely due to high flow velocities inhibiting bed coarsening in floods and fine-sediment deposition increasing resistance in dry periods. This nonlinear response indicates that neglecting seasonal coupling of water-sediment processes will lead to stage prediction biases, especially in downstream reaches affected by Dongting Lake backwater (e.g., a confidence bandwidth of 1.2 m at Jianli Station).

This study introduces a novel scenario-based decomposition framework that advances the mechanistic understanding of stage-discharge relationship evolution in regulated rivers. The principal innovation lies in the quantitative isolation of coupled geomorphic impacts through a structured methodology combining four distinct scenarios (Table 3) with a stratified difference approach. Specifically, by strategically contrasting scenarios with fixed/dynamic topography (D_1/D_2) and roughness (n_1/n_2), we effectively decouple the individual contributions of bed incision ($\Delta Zt = ZX1 - ZX2$) and roughness variation ($\Delta Zn = ZX1 - ZX3$), overcoming the limitation of traditional analyses that treat these factors

as interdependent. This approach enables spatiotemporally explicit quantification of factor dominance, revealing—for the first time—that incision controls >80% of stage reduction at upstream stations (e.g., Zhicheng) while roughness contributes >50% to stage rise downstream (e.g., Jianli). The framework, validated via the Fourier Amplitude Sensitivity Test, provides a transferable paradigm for diagnosing complex hydro-geomorphic feedbacks in global reservoir-affected rivers, moving beyond qualitative correlation to predictive, causality-driven management.

Compared with international cases like the Mississippi and Rhine Rivers, this study identifies a unique mechanism in the Jingjiang River's topography-roughness feedback [34]. Clear-water erosion triggered by the TGR caused widespread bed coarsening (roughness increased from 0.023–0.028 to 0.027–0.035), but morphological adjustments in downstream meandering reaches (e.g., drastic migration in Jiepai Section) amplified uncertainty in roughness variability [35]. This contrasts with findings from Egypt's Nile River—where straight channel geometry led to uniform roughness impacts on water levels—underscoring channel morphology's control over factor contributions [36].

The one-dimensional hydrodynamic model and layered difference method employed in this study, while effective in revealing macro-scale spatiotemporal differentiation patterns in the influence of topography and roughness, still exhibit three main limitations: (1) The one-dimensional model framework simplifies the two-/three-dimensional flow structures in complex river reaches (e.g., high-sinuosity segments and confluence zones), failing to resolve key processes such as lateral circulation; (2) Although the layered difference method achieves decoupling, its depiction of nonlinear interactions among factors remains relatively coarse; (3) The current scenario design primarily focuses on the coupling of topography and roughness, without fully incorporating direct influences of dynamic hydraulic factors such as backwater effects from Dongting Lake and tributary inflows.

To advance beyond the current findings, future studies may follow these operational pathways:

1. Development of a Coupled Model System: Construct a 1D-2D coupled hydrodynamic and sediment transport model, embedding 2D detailed models in key areas within long-reach 1D simulations to explicitly capture two-dimensional hydrodynamic processes.
2. Deepening Multi-Factor Interaction Simulations: Introduce dynamic boundary conditions (e.g., backwater effects and flow diversion ratios) into scenario designs, and utilize sensitivity analysis or response surface methodology to quantify synergistic effects of multiple factors (topography + roughness + hydrodynamics).
3. Integration of High-Frequency Data and Data Assimilation Techniques: Combine high-frequency monitoring data (e.g., ADCP and remote sensing) with data assimilation algorithms (e.g., ensemble Kalman filter) to dynamically optimize key parameters like roughness, thereby enhancing the model's real-time prediction capability.

5. Conclusions

This study constructed a 1D hydrodynamic model to quantitatively separate the contributions of Bed erosion and roughness changes to the stage-discharge relationship in the Jingjiang River reach. While previous studies have often focused on the isolated effects of either geometric adjustment or roughness changes, a key distinction of our work lies in its novel framework that enables the synchronous quantification and coupling of both factors. More importantly, this approach allows for the quantitative separation of their individual contribution rates across different time periods and flow regimes, thereby revealing the spatiotemporal heterogeneity of their synergistic effects for the first time in this regulated reach. The results indicate that: topographic changes dominate the water

level drop at the upstream section (e.g., a decrease of 1.7 m at a discharge of 5000 m^3/s at the Zhicheng Station), and the relationship curve exhibits a convergent trend, with a contribution rate exceeding 80%; conversely, roughness changes significantly amplify water-level rise downstream (e.g., a 0.7 m rise at the same discharge at Jianli Station). The coupling effect of these factors drives a spatial differentiation of "decline upstream but stabilization downstream" along the entire reach, with the effect offsetting even observed in the medium-low flow range (15,000–20,000 m^3/s) at Jianli Station.

Temporally, the topographic contribution rate exhibits a downstream attenuation pattern spatially. While roughness contributions turn negative in dry seasons (November) due to fine-sediment deposition. Spatially, channel morphology (e.g., a sinuosity coefficient of 3.0 in the Lower Jingjiang) amplifies roughness sensitivity, leading to higher prediction uncertainty downstream (confidence bandwidth: 1.2 m) than upstream.

These findings offer practical implications for flood control and navigation management in the Jingjiang Reach. The quantified impacts of post-dam channel adjustments provide critical operational guidance for the Jingjiang Reach: upstream (e.g., Zhicheng to Shashi), where bed erosion dominates, periodic updates of stage-discharge rating curves—especially vital for low-flow navigation management should be implemented; while downstream (e.g., below Jianli), where roughness exhibits high interannual variability, flood prevention plans must integrate systematic monitoring of bed material composition and dune morphology as corrective parameters in forecasting models. The increase in bed roughness induced by channel coarsening directly threatens navigation safety by amplifying water-depth variability, particularly in high-sinuosity stretches where low-flow stage fluctuations increase grounding risks, and it also raises water stages for a given discharge in wide-shallow downstream segments, challenging existing levee standards. Notably, the observed "negative roughness contribution" following floods signals a temporary resistance reduction due to fine sediment deposition, which may create a false sense of safety before subsequent erosion abruptly restores high roughness. Therefore, a spatially differentiated management framework is essential: the upper reach should leverage the relatively stable topographic incision effect for stage forecasting, whereas the lower reach requires dynamic roughness monitoring (e.g., bed material sampling and ADCP surveys) integrated into early-warning systems—collectively demonstrating how the "topography–roughness–channel morphology" coupling mechanism offers a universal methodology for predicting stage–discharge relationships in reservoir-regulated rivers worldwide.

Author Contributions: Methodology, D.Z.; Software, D.Z.; Data curation, Y.C.; Supervision, M.D.; Project administration, Y.L.; Funding acquisition, M.D. All authors have read and agreed to the published version of the manuscript.

Funding: This research was funded by Hubei Provincial Natural Science Foundation grant number 2024AFD354 and National Key Research and Development Program of China grant number 2022YFC3202801; The APC was funded by [2024AFD354].

Data Availability Statement: Dataset available on request from the authors. The raw data supporting the conclusions of this article will be made available by the authors on request.

Conflicts of Interest: The authors declare no conflict of interest.

Abbreviations

The following symbols are used in this paper:

RE	Relative Error
NSE	Nash-Sutcliffe Efficiency coefficient
D1	1996 surveyed topography
D2	2021 surveyed topography
n1	1996 bed roughness coefficient
n2	2021 bed roughness coefficient
ΔZt	water level decrease induced by bed erosion
ΔZn	water level increase induced by bed coarsening
ZX1	water level under Scenario 1 (pre-dam conditions)
ZX2	water level under Scenario 2 (post-dam topography with pre-dam roughness)
ZX3	water level under Scenario 3 (pre-dam topography with increased roughness)
ZX4	water level under Scenario 4 (coupled post-dam changes)
ΔZtotal	total water level change under combined geo- and roughness-change effects Geotopographic change
Rou	roughness change
FAST	Fourier Amplitude Sensitivity Test

References

1. Shao, Q.; Dutta, D.; Karim, F.; Petheram, C. A method for extending stage-discharge relationships using a hydrodynamic model and quantifying the associated uncertainty. *J. Hydrol.* **2018**, *556*, 154–172. [CrossRef]
2. Piadeh, F.; Behzadian, K.; Alani, A.M. A critical review of real-time modelling of flood forecasting in urban drainage systems. *J. Hydrol.* **2022**, *607*, 127476. [CrossRef]
3. Hein, T.; Hauer, C.; Schmid, M.; Stöglehner, G.; Stumpp, C.; Ertl, T.; Graf, W.; Habersack, H.; Haidvogl, G.; Hood-Novotny, R.; et al. The coupled socio-ecohydrological evolution of river systems: Towards an integrative perspective of river systems in the 21st century. *Sci. Total Environ.* **2021**, *801*, 149619. [CrossRef]
4. Stephens, C.M.; Lall, U.; Johnson, F.M.; Marshall, L.A. Landscape changes and their hydrologic effects: Interactions and feedbacks across scales. *Earth Sci. Rev.* **2021**, *212*, 103466. [CrossRef]
5. Wu, Q.; Ke, L.; Wang, J.; Pavelsky, T.M.; Allen, G.H.; Sheng, Y.; Duan, X.; Zhu, Y.; Wu, J.; Wang, L.; et al. Satellites reveal hotspots of global river extent change. *Nat. Commun.* **2023**, *14*, 1587. [CrossRef]
6. Xia, J.; Deng, S.; Lu, J.; Xu, Q.; Zong, Q.; Tan, G. Dynamic channel adjustments in the Jingjiang Reach of the Middle Yangtze River. *Sci. Rep.* **2016**, *6*, 22802. [CrossRef]
7. Yang, X.; Sun, Z.; Li, Y.; Deng, J.; Xiong, H.; Li, D. Mechanisms of bar adjustments in the Jingjiang Reach of the Yangtze River in response to the operation of the Three Gorges Dam. *J. Hydrol.* **2023**, *616*, 128802. [CrossRef]
8. Alomari, N.K.; Yusuf, B.; Mohammad, T.A.; Ghazali, A.H. Experimental investigation of scour at a channel junctions of different diversion angles and bed width ratios. *Catena* **2018**, *166*, 10–20. [CrossRef]
9. Yang, Y.; Zhang, M.; Zhu, L.; Liu, W.; Han, J.; Yang, Y. Influence of Large Reservoir Operation on Water-Levels and Flows in Reaches below Dam: Case Study of the Three Gorges Reservoir. *Sci. Rep.* **2017**, *7*, 15640. [CrossRef] [PubMed]
10. Dallmann, J.; Phillips, C.B.; Teitelbaum, Y.; Saavedra Cifuentes, E.Y.; Sund, N.; Schumer, R.; Arnon, S.; Packman, A.I. Bedform segregation and locking increase storage of natural and synthetic particles in rivers. *Nat. Commun.* **2021**, *12*, 7315. [CrossRef]
11. Li, P.; Wang, J.; Hu, K.; Xie, J. Shedding effects of sediment composition and bed morphology on debris flow dynamics and entrainment mechanism: Insights from laboratory experiments. *Eng. Geol.* **2024**, *333*, 107495. [CrossRef]
12. Tian, J.; Chang, J.; Zhang, Z.; Wang, Y.; Wu, Y.; Jiang, T. Influence of Three Gorges Dam on Downstream Low Flow. *Water* **2019**, *11*, 65. [CrossRef]
13. Lyu, Y.; Fagherazzi, S.; Tan, G.; Zheng, S.; Feng, Z.; Han, S.; Shu, C. Hydrodynamic and geomorphic adjustments of channel bars in the Yichang-Chenglingji Reach of the Middle Yangtze River in response to the Three Gorges Dam operation. *Catena* **2020**, *193*, 104628. [CrossRef]
14. Nones, M.; Guo, C. Remote sensing as a support tool to map suspended sediment concentration over extended river reaches. *Acta Geophysica* **2025**, *73*, 4655–4668. [CrossRef]
15. Larsen, I.J.; Montgomery, D.R. Landslide erosion coupled to tectonics and river incision. *Nat. Geosci.* **2012**, *5*, 468–473. [CrossRef]
16. Liao, Y.; Yuan, Z.; Zhuo, M.; Huang, B.; Nie, X.; Xie, Z.; Tang, C.; Li, D. Coupling effects of erosion and surface roughness on colluvial deposits under continuous rainfall. *Soil Tillage Res.* **2019**, *191*, 98–107. [CrossRef]

17. Shen, E.; Liu, G.; Zhang, Q.; Dan, C.; Liu, C.; Li, H.; Liu, Y.; Qu, X.; Xia, X.; Liu, D.; et al. Exploring coupling effects of rainfall and surface roughness on the sheet flow velocity. *Int. Soil Water Conserv. Res.* **2025**, *13*, 164–176. [CrossRef]
18. Wang, C.; Li, Y.; Li, Y.; Fan, Y.; Feng, Z. Coupling effect of large deformation and surface roughness on dynamic frictional contact behaviors of hyperelastic material. *Comput. Mech.* **2025**, *75*, 455–473. [CrossRef]
19. Zhang, W.; Wang, W.-g.; Zheng, J.-h.; Wang, H.-g.; Wang, G.; Zhang, J.-s. Reconstruction of stage–discharge relationships and analysis of hydraulic geometry variations: The case study of the Pearl River Delta, China. *Global Planet. Change* **2015**, *125*, 60–70. [CrossRef]
20. Kona Sai, V.; Das Bhowmik, R. Understanding the Interannual Variation in the River Stage–Discharge Relationship and Its Impact on Flood Discharge Estimation. *J. Hydrol. Eng.* **2025**, *30*, 04025020. [CrossRef]
21. Baiamonte, G. Dimensionless Stage-Discharge Relationship for a Non-Linear Water Reservoir: Theory and Experiments. *Hydrology* **2020**, *7*, 23. [CrossRef]
22. Gomes, M.N.; Rápalo, L.M.C.; Oliveira, P.T.S.; Giacomoni, M.H.; do Lago, C.A.F.; Mendiondo, E.M. Modeling unsteady and steady 1D hydrodynamics under different hydraulic conceptualizations: Model/Software development and case studies. *Environ. Model. Softw.* **2023**, *167*, 105733. [CrossRef]
23. Lin, B.; Wicks, J.M.; Falconer, R.A.; Adams, K. Integrating 1D and 2D hydrodynamic models for flood simulation. *Proc. Inst. Civ. Eng. Water Manag.* **2006**, *159*, 19–25. [CrossRef]
24. Teng, J.; Jakeman, A.J.; Vaze, J.; Croke, B.F.W.; Dutta, D.; Kim, S. Flood inundation modelling: A review of methods, recent advances and uncertainty analysis. *Environ. Model. Softw.* **2017**, *90*, 201–216. [CrossRef]
25. Asselman, N.E.M.; Wijngaarden, M.v. Development and application of a 1D floodplain sedimentation model for the River Rhine in The Netherlands. *J. Hydrol.* **2002**, *268*, 127–142. [CrossRef]
26. Ma, H.; Nittrouer, J.A.; Fu, X.; Parker, G.; Zhang, Y.; Wang, Y.; Wang, Y.; Lamb, M.P.; Cisneros, J.; Best, J.; et al. Amplification of downstream flood stage due to damming of fine-grained rivers. *Nat. Commun.* **2022**, *13*, 3054. [CrossRef]
27. Pan, D.; Zhang, Y.; Liu, S.; Zhang, Z. Advancing evolution characterization in dynamic networks: A quantum walk and thermodynamics perspective. *Pattern Recognit.* **2025**, *165*, 111630. [CrossRef]
28. Tang, F.; Fu, M.; Wang, L.; Song, W.; Yu, J.; Wu, Y. Dynamic evolution and scenario simulation of habitat quality under the impact of land-use change in the Huaihe River Economic Belt, China. *PLoS ONE* **2021**, *16*, e0249566. [CrossRef] [PubMed]
29. Han, D.; Yu, D.; Qiu, J. Assessing coupling interactions in a safe and just operating space for regional sustainability. *Nat. Commun.* **2023**, *14*, 1369. [CrossRef]
30. Tansar, H.; Babur, M.; Karnchanapaiboon, S.L. Flood inundation modeling and hazard assessment in Lower Ping River Basin using MIKE FLOOD. *Arabian J. Geosci.* **2020**, *13*, 934. [CrossRef]
31. Wan, X.; Xu, G.; Zhang, Q.; Tse, P.W.; Tan, H. A quantitative method for evaluating numerical simulation accuracy of time-transient Lamb wave propagation with its applications to selecting appropriate element size and time step. *Ultrasonics* **2016**, *64*, 25–42. [CrossRef] [PubMed]
32. Zou, Y.; Yan, B.; Feng, B.; Zhang, J.; Tang, Y. A Three-Parameter Hydrological Model for Monthly Runoff Simulation—A Case Study of Upper Hanjiang River Basin. *Water* **2023**, *15*, 474. [CrossRef]
33. Yang, J.; Wen, L.; Guo, J.; Chen, Y.; Zhu, Y.; Wang, Y.; Ma, M. A cooperative search algorithm-based flood forecasting framework: Application across diverse Chinese catchments. *Front. Earth Sci.* **2025**, *13*, 1538235. [CrossRef]
34. Hudson, P.F.; Middelkoop, H.; Stouthamer, E. Flood management along the Lower Mississippi and Rhine Rivers (The Netherlands) and the continuum of geomorphic adjustment. *Geomorphology* **2008**, *101*, 209–236. [CrossRef]
35. Lingling, Z.H.U.; Xia, Y.; Quanxi, X.U. Response of low water level change to bed erosion and the operation of Three Gorges Reservoir in upper Jingjiang reach. *Acta Geogr. Sin.* **2017**, *72*, 1184–1194. [CrossRef]
36. Acquafredda, V. A Look into the Historical Depths of the Nile Waters: What to Learn from History. In *Nile and Grand Ethiopian Renaissance Dam: Past, Present and Future*; Melesse, A.M., Abtew, W., Moges, S.A., Eds.; Springer International Publishing: Cham, Switzerland, 2021; pp. 9–33.

Disclaimer/Publisher's Note: The statements, opinions and data contained in all publications are solely those of the individual author(s) and contributor(s) and not of MDPI and/or the editor(s). MDPI and/or the editor(s) disclaim responsibility for any injury to people or property resulting from any ideas, methods, instructions or products referred to in the content.